JOURNAL OF ENVIRONMENTAL SCIENCES 151 (2025) 441–453

Available online at www.sciencedirect.com

ScienceDirect

www.elsevier.com/locate/jes

JES JOURNAL OF ENVIRONMENTAL SCIENCES

www.jesc.ac.cn

Research Article

Ozone risk assessment of common cypress (*Cupressus sempervirens* L.) clones and effects of *Seiridium cardinale* infection

Jacopo Manzini[1,2], *Yasutomo Hoshika*[1,*], *Roberto Danti*[3], *Barbara Baesso Moura*[1], *Elena Paoletti*[1], *Gianni Della Rocca*[3]

[1] *Institute of Research on Terrestrial Ecosystems (IRET), National Research Council of Italy (CNR), Via Madonna del Piano 10, Sesto Fiorentino 50019, Italy*

[2] *Department of agricultural, food, environmental and forestry science and technology (DAGRI), University of Florence, Piazzale delle Cascine, 18, Firenze 50144, Italy*

[3] *Institute for Sustainable Plant Protection (IPSP), National Research Council of Italy (CNR), Via Madonna del Piano 10, Sesto Fiorentino 50019, Italy*

ARTICLE INFO

Article history:
Received 4 December 2023
Revised 11 March 2024
Accepted 13 March 2024
Available online 22 March 2024

Keywords:
Abiotic stress
Air pollution
Ozone risk assessment
Plant pathology
PODy
Stomatal conductance model

ABSTRACT

Cupressus sempervirens is a relevant species in the Mediterranean for its cultural, economic and landscape value. This species is threatened by *Seiridium cardinale*, the causal agent of the cypress canker disease (CCD). The effects of biotic stressors on O_3 risk assessment are unknown and a comprehensive O_3 risk assessment in *C. sempervirens* is missing. To fill these gaps, two clones of *C. sempervirens*, one resistant (Clone R) and one susceptible to CCD (Clone S), were subjected to three levels of O_3 (Ambient Air - AA; 1.5 × AA; 2.0 × AA) for two consecutive years in an O_3-free-air controlled exposure facility and artificially inoculated with *S. cardinale*. Both the exposure- (AOT40) and flux-based (PODy) indices were tested. We found that PODy performed better than AOT40 to assess O_3 effects on biomass and the critical level for a 4% biomass loss was 2.51 mmol/m^2 POD_2. However, significant O_3 dose-response relationships were not found for the inoculated cypresses because the combination of middle level O_3 (1.5 × AA) and inoculation stimulated a biomass growth in Clone S as hormetic response. Moreover, we found a different inter-clonal response to both stressors with a statistically significant reduction of total and belowground biomass following O_3, and lower root biomass in Clone S than in Clone R following pathogen infection. In summary, Clone R was more resistant to O_3, and inoculation altered O_3 risk via an hormetic effect on biomass. These results warrant further studies on how biotic stressors affect O_3 responses and risk assessment.

* Corresponding author.
E-mail: yasutomo.hoshika@cnr.it (Y. Hoshika).

https://doi.org/10.1016/j.jes.2024.03.026

Introduction

Climate change is mainly due to the release of greenhouse gases (CO_2, CH_4 and N_2O) into the atmosphere by anthropogenic activities (Naz et al., 2022), is threatening plant species and causing abiotic stresses (Chaudhry and Sidhu, 2022). Both rising temperature and solar radiation induce direct physiological stress on plants (Dusenge et al., 2019; Roeber et al., 2021) and also promote an increase in tropospheric concentrations of ozone (O_3), a secondary pollutant with a phytotoxic effect (Grulke and Heath, 2020). Ozone is a strong seasonal oxidant in Mediterranean areas typically linked to the high irradiance and temperature that occur during summer months (Paoletti, 2006; Ochoa-Hueso et al., 2017) with an annual average of about 40–50 ppb (Sicard et al., 2017; Jiang et al., 2020). Ozone causes direct damage to plants (i.e., biomass loss, foliar injury and defoliation) due to alteration of biochemical and physiological functions and may enhance susceptibility to other abiotic factors e.g. drought (Hayes et al., 2015) or parasitic diseases (Ahmed, 2007).

The assessment of O_3 risk to vegetation is based on the definition of critical levels (CLs) specified as O_3 cumulative exposure or flux thresholds able to induce a biomass reduction of 5% or 4%, respectively (CLRTAP, 2017). Currently, AOT40 (Accumulated exposure Over an hourly Threshold of 40 ppb) is the index used to detect CLs for forest protection in Europe (European Council Directive, 2008) but the phytotoxic O_3 dose above an hourly threshold y of uptake (PODy) is considered a more suitable and realistic metric for risk assessment as is based on the amount of O_3 effectively absorbed by leaves through stomatal opening (CLRTAP, 2017; Paoletti et al., 2022). In addition, climate change has potentially dramatic consequences on biotic stress factors (Zandalinas et al., 2021) as it may induce sudden and significant variations in thermal and pluviometric regimes thus affecting life cycles of plant parasites and altering their rate of growth, survival, reproduction, pathogenicity and spread in the environment (Della Rocca et al., 2019a). Therefore, the study of interactions between biotic and abiotic stressors and their effect on eco-physiological alterations in plants is of particular interest (Trivedi et al., 2022). Defense mechanisms against O_3-induced oxidative stress are similar to those against some pathogen attacks through various physiological and molecular cross-talking pathways (Kangasjärvi et al., 2005; Vainonen and Kangasjärvi, 2015). However, it is not clear whether simultaneous stresses can be antagonistic, synergistic or additive (Ben Rejeb et al., 2014) and, to the best of our knowledge, it is still unknown if biotic stressors may affect the O_3 risk assessment in plants.

Common cypress (*Cupressus sempervirens* L.) is a widespread tree species in the Mediterranean basin and an iconic element of its landscape and culture (Farahmand, 2020). The sensitivity to O_3 in this species has not been investigated yet while the effects of fungal pathogen *Seiridium cardinale* (Wagener) Sutton et Gibson, that is the aetiological agent of Cypress Canker Disease (CCD), are widely studied (Graniti, 1998; Della Rocca et al., 2011a, 2013; Danti et al., 2013a, 2018; Della Rocca et al., 2019b). The pathogen was introduced in Europe at the beginning of the 20th century (Danti and Della Rocca, 2017) and, since the '70s, millions of trees were killed by CCD epidemics especially in Italy and Greece where the incidence exceeded 50% in some areas of Tuscany and the Peloponnese (Graniti, 1998; Danti et al., 2013a; Danti and Della Rocca, 2017). Among the various strategies developed to counteract CCD, genetic improvement is the most effective (Raddi and Panconesi, 1981; Danti et al., 2011, 2013b). Since the '70s, Italy began a genetic improvement programme by selecting and/or crossing cypress genotypes able to react to the infection and heal the bark lesion caused by the pathogen, thus selecting and patenting clones that are resistant or poorly susceptible to the disease (Panconesi and Raddi, 1991; Danti et al., 2006, 2013b).

We employed two cypress clones characterized by different susceptibility to CCD, two-year fumigation in an O_3 Free-Air Controlled Exposure (FACE) facility, an artificial inoculation with *S. cardinale*, using AOT40 and PODy as metrics of risk assessment. We hypothesized that CCD susceptible and tolerant clones may respond differently to O_3 and that *S. cardinale* infection may affect O_3 risk assessment in *C. sempervirens*.

1. Materials and methods

1.1. Plant material

The experiment lasted 17 months (from May 2019 to October 2020) and was carried out on two clones of *C. sempervirens*, one resistant to CCD (clone R - PM 2546) and another one susceptible to CCD (clone S - PM 3375). Clone R shows a columnar crown, while clone S is characterized by an intermediate *habitus*. Cypress ramets belonged to the cypress germplasm collection of the Institute of Plant Sustainable Protection of the Italian National Research Council (IPSP-CNR) and were obtained by grafting on unselected cypress rootstock. At the beginning of the experiment, ramets were 2-year-old from grafting and the average height was 72.4 ± 1.15 cm for clone R, and 65.6 ± 1.23 cm for clone S. The cypresses were hosted in 25-L pots (⌀ 35 cm) containing 50% peat and 50% pumice with the addition of 3.3 kg/m^3 of slow-release rate granular fertilizer (Basacote Plus 12M®) and 6 kg/m^3 of Leonardite. Drip irrigation of 500 ± 50 mL/day for each pot was provided throughout the main growing seasons (May-October) to hold field capacity.

1.2. Ozone face fumigation set-up

The FO_3X facility (Free air O_3 eXposure), located in Sesto Fiorentino, Florence, Italy (43°48′59″ N, 11° 12′01″ E, 55 m a.s.l.) was used to perform O_3 fumigation of the cypress clones. FO_3X is one of the six O_3-FACEs currently available in the world (Montes et al., 2022), the only one representative of the Mediterranean climate. Cypress clones were exposed to three levels of O_3 concentrations: ambient air (AA), one and a half time the concentration of O_3 in AA (1.5 ×) and two times the O_3 concentration in AA (2.0 ×). As reported by Paoletti et al. (2017), FO_3X is made up of three replicated square plots (5 m × 5 m) for each O_3 level. Ozone is generated from pure oxygen by an O_3 generator (TGOC13X, Triogen Ltd., Glasgow, UK) and then

diluted with ambient air in a mixing tank and injected by 25 Teflon tubes hanging from a fixed grid above the plants (2 m high) in each plot.

A total of 72 cypress ramets (36 per clone) were fumigated. Each plot (three for each O_3 level) hosted 8 ramets: 4 of clone R and 4 of clone S. Exposure to the three levels of O_3 was continuously maintained between May and October during both growing seasons (2019 and 2020). Environmental data of air temperature (T), relative humidity (RH), photosynthetic active radiation (PAR) and wind speed were recorded by a Watchdog station (Mod. 2000; Spectrum Technology, Inc., Aurora, IL, USA) placed at 2.5 m a.g.l.

1.3. *Pathogen inoculation and bark lesion measurement*

The artificial stem inoculation of both cypress clones with the bark pathogen *S. cardinale* was carried out on June 1st 2020 after one year of growth. The ATCC 38654 standard reference isolate of *S. cardinale* was used for the inoculations. The pathogen was grown in Petri dishes on PDA (Potato Dextrose Agar) substrate for 15 days at 25°C in the dark. For each O_3 treatment (AA, 1.5 × , 2.0 ×), half of the ramets in each plot was inoculated for a total of 12 ramets (6 of clone R and 6 of clone S). Two simultaneous inoculations were performed on the trunk of each ramet. The first one was about 10 cm above the grafting point and the second one was 20 cm above the previous inoculation. Inoculations were accomplished as described in Della Rocca et al. (2018) and a circular wound (diameter 0.5 cm) was performed by removing a portion of the bark down to the woody tissue using a cork borer. Then, a plug of *S. cardinale* mycelium of equal size was removed from a Petri dish and inserted into the wound. The inoculations were covered with moistened cotton wool wrapped with parafilm to ensure the right humidity conditions and maximize the infection success. Maximum length and width of the resulting bark lesions were measured at the end of the experiment and their surface area (cm^2) was calculated with the following formula: [(Canker height/2) × (Canker width/2)] × π (Della Rocca et al., 2011b). The average of the two lesions of each ramet was considered.

1.4. *Biomass assessment*

Biomass of cypress clones was evaluated at the beginning (B_{start}), in an additional subset of ramets of both clones ($n = 6$), and at the end of the experiment (B_{end}). In October 2020, each plant was harvested and subdivided in above- (stems and twigs) and below-ground biomass (coarse and fine roots). Then, each part was dried for 5 days in an oven at 70°C until constant weight and assessed separately by an analytical balance (Sartorius, Germany). The final biomass growth (B_{final}) was obtained as difference between B_{end} and B_{start}.

1.5. *Stomatal conductance measurements and modelling*

Stomatal conductance (g_{sto}) measurements were carried out by a portable infrared gas analyzer (LI-6800, Li-Cor Inc. Lincoln, NE, USA) equipped with a cuvette for hardwoods with a circular opening of 2 cm^2. As cypress is a conifer, parameters returned by the instrument were re-proportioned to the actual leaf surface placed in the cuvette. The effective leaf area of cypress twigs was obtained using the Easy Leaf Area Free application (Easlon and Bloom, 2014). Two types of g_{sto} measurement were carried out. For the measurement under light-saturated conditions, the following parameters were set: 1500 µmol/(m^2·sec) for the photosynthetic photon flux density (PPFD), 400 µmol/mol as ambient CO_2 concentration (Ca) and 25°C as leaf temperature. The light-saturated measurements were made on 26th May, 29–30th June, 20th August and 5th October 2020. In addition, further measurements were made under various natural environmental conditions of T, RH and PPFD by setting the leaf cuvette to the track-ambient mode. These measurements with natural environmental conditions were conducted on 22–23th July, 19–20th September 2019 and 6–7th, 17–26th February 2020. A final database of 198 and 204 measurements of g_{sto} for Clone R and Clone S, respectively, was used to estimate the parameters of the stomatal conductance model based on Jarvis (1976) multiplicative algorithm. According to the model, g_{sto} was described as:

$$g_{sto} = g_{max} \times f_{light} \times \max\{f_{min},\ (f_{temp} \times f_{VPD} \times f_{phen} \times f_{O3} \times f_{canker})\} \quad (1)$$

where, g_{max} (mmol O_3/(m^2·sec)) and f_{min} (fraction) are the maximum and minimum stomatal conductance (95th and 5th percentiles of all g_{sto} data, respectively), while the other functions are limiting factors scaled from 0 to 1. In detail, f_{light}, f_{temp}, f_{VPD}, f_{phen}, f_{O3}, f_{canker} depended on photosynthetically relevant photon flux density at the leaf surface (PPFD, µmol photons/(m^2·sec)), air temperature (T, °C), vapor pressure deficit (VPD, kPa), phenology (Day of the year – DOY), O_3 (nmol/mol) and canker lesion extension in the bark (cm^2) around the inoculation point, respectively. The stomatal response to PPFD was specified as:

$$f_{light} = 1 - \exp(-a \times \text{PPFD}) \quad (2)$$

where, a is a species-specific parameter defining the shape of the exponential relationship, PPFD (µmol photons/(m^2·sec)) is photosynthetically relevant photon flux density at the leaf surface.

The air temperature function (f_{temp}) considered the optimum (T_{opt}), minimum (T_{min}), and maximum temperature (T_{max}) for g_{sto}, and it was expressed as:

$$f_{temp} = \left(\frac{T - T_{min}}{T_{opt} - T_{min}}\right)\left\{\left(\frac{T_{max} - T}{T_{max} - T_{opt}}\right)^{\left(\frac{T_{max} - T_{opt}}{T_{opt} - T_{min}}\right)}\right\} \quad (3)$$

The response of g_{sto} to vapor pressure deficit (VPD, kPa) was given by the following function:

$$f_{VPD} = \min\left[1,\ \max\left\{f_{min}, \left(\frac{(1 - f_{min}) \times (VPD_{min} - VPD)}{(VPD_{min} - VPD_{max})}\right) + f_{min}\right\}\right] \quad (4)$$

where, VPD_{min} and VPD_{max} indicate the threshold of VPD for attaining minimum and maximum stomatal opening, respectively. If VPD > VPD_{min} then f_{VPD} is set to f_{min}. If VPD < VPD_{max} then f_{VPD} is 1. According to Emberson et al. (2000) the stomatal

response to phenology was described as:

$$\begin{aligned} f_{phen} &= (1 - f_{phen\_c}) \times ((DOY - A_{start})/f_{phen\_a}) + f_{phen\_c} \\ &\quad \text{when } A_{start} \le DOY < (A_{start} + f_{phen\_a}), \\ f_{phen} &= 1 \text{ when } (A_{start} + f_{phen\_a}) \le DOY \le (A_{end} - f_{phen\_b}), \\ f_{phen} &= (1 - f_{phen\_d}) \times ((A_{end} - DOY)/f_{phen\_b}) + f_{phen\_d} \\ &\quad \text{when } (A_{end} - f_{phen\_b}) < DOY \le A_{end} \end{aligned} \quad (5)$$

where, DOY is the day of year, A_{start} and A_{end} represented the start (1st January) and the end (31st December) of the leafy period. The functions f_{phen_a} and f_{phen_b} are the number of days of f_{phen} to reach its maximum and minimum respectively while f_{phen_c} and f_{phen_d} represent the maximum fraction of f_{phen} at A_{start} and A_{end}.

Considering that O_3 concentration may affect the reduction of g_{sto} we enclosed in our model the following function (f_{O3}) previously proposed by Hoshika et al. (2018a):

$$f_{O3} = 1 - q \times [O_3] \quad (6)$$

where, q reflects stomatal sensitivity to O_3 concentration, and $[O_3]$ (ppb) is hourly mean O_3 concentration. Moreover, we innovatively suggested a new function (f_{canker}) that considers g_{sto} responses to necrotic canker lesion surface as *S. cardinale* affects cortical tissues also altering water flow in infected branches (Madar et al., 1990). It was calculated as:

$$f_{canker} = c(C_S)^2 - k(C_S) + 1 \quad (7)$$

where, C_S (cm^2) is the average canker surface, while c and k are two constant factors.

f_{light}, f_{temp}, f_{VPD}, f_{phen}, f_{O3} were estimated using a boundary line analysis (Braun et al., 2010; Hoshika et al., 2012, 2018b), while f_{canker} was obtained by a quadratic regression.

To test the performance of the model, we correlated the measured and estimated values of g_{sto} using the baseline model that considered f_{light}, f_{temp}, f_{VPD} and f_{phen} or by adding only the ozone (f_{O3}) or canker (f_{canker}) function or both.

1.6. Ozone metrics calculation: AOT40 and PODy

According to the Convention on Long-range Transboundary Air Pollution (CLRTAP, 2015), AOT40 was calculated as the sum of the excess of hourly concentrations over a threshold of 40 ppb during daylight hours characterized by short wave radiation > 50 W/m^2. Conversely, POD_y was estimated during the experimental period (from May 2019 to October 2020) as:

$$POD_y = \int \max(F_{st} - Y, 0) \cdot dt \quad (8)$$

where, Y is a species-specific threshold of the hourly stomatal O_3 flux, and F_{st} (nmol/(m^2·sec)) is calculated as:

$$F_{st} = [O_3] \times g_{sO3} \times r_c/(r_b + r_c) \quad (9)$$

where, $[O_3]$ (ppb) is the hourly O_3 concentration; g_{sO3} (mol O_3/(m^2·sec)) is g_{sto} multiplied for 0.663, a factor that considers the ratio of diffusivities between O_3 and water vapor (CLRTAP, 2015); r_c is the leaf surface resistance $r_c = 1/g_{sto} + g_{ext}$ (g_{ext} = 0.0164 mol O_3/(m^2·sec)); r_b is the leaf boundary layer resistance (sec/m) calculated as $r_b = 1.3 \times 150 \times (L_d/u)^{0.5}$ where u is the wind speed (m/sec), L_d is the cross-wind leaf dimension (0.008 m for conifers, CLRTAP, 2017) and the factor 1.3 accounted for differences in diffusivity between heat and O_3 (CLRTAP, 2015). Aerodynamic resistance (r_a) was not considered as O_3 concentration was measured at plant height. Different PODy detoxification thresholds (y = 0–5 nmol O_3/(m^2·sec)) were tested to identify the best PODy index to predict O_3 effects on cypress biomass. AOT40 and PODy were obtained by summing 2019 and 2020 values.

1.7. Data analysis

We calculated a control reference biomass (B_{ref}) for the risk assessment as proposed by Paoletti et al. (2017), assuming an O_3 concentration of 10 ppb as daily average in the pre-industrial clean air as suggested by Fowler (2008). Then we assessed the relative biomass (B_{rel}) as the ratio between the biomass at the end of the experimental period (B_{final}) and the reference biomass: $B_{rel} = B_{final}/B_{ref}$.

We analyzed the Y-axis intercept with its confidence interval (C.I.) and the R^2 value of each linear regression between B_{rel} (with Y-axis intercept = 1 considered as total biomass in pre-industrial atmosphere) and the exposure- (AOT40) and flux-based (POD_y) values. Then, to select the most suitable index and calculate the CLs, we employed these two objective criteria. Firstly, C.I. had to include Y-intercept = 1 (Büker et al., 2015). Secondly, the highest R^2 value was selected from the equations that consider the first criterion (Hoshika et al., 2018c). The CLs were evaluated as 4% biomass loss, according to CLRTAP (2017).

Data of B_{final} (total, aboveground or belowground biomass) were averaged per plot (n = 3) and, after checking for normal distribution (Kolmogorov-Smirnov test) and homogeneity of variance (Levene's test), differences between clones, O_3 treatments and inoculation were tested by means of three-way ANOVA by using Rstudio software.

Finally, the goodness of fit for g_{sto} model with each combination of functions was tested by the R^2 value and the root mean square error (RMSE).

2. Results

2.1. Meteorological conditions and O_3 exposure

Average daily air temperature during the experimental period was 22.76 ± 0.37°C for 2019 and 22.24 ± 0.40°C for 2020 (Fig. 1A). Daily average VPD was 1.55 ± 0.02 kPa in 2019 and 1.33 ± 0.06 kPa in 2020, while average PAR was 46.28 ± 1.20 mol/(m^2·day) in 2019 and 39.09 ± 1.55 mol/(m^2·day) in 2020. Accumulated precipitation was lower in 2019 (161.3 mm) than in 2020 (270.1 mm). Daily mean air O_3 concentrations, considering both years, were 38.51 ± 0.72, 54.69 ± 1.13 and 71.49 ± 1.50 ppb at AA, 1.5 × and 2.0 × , respectively, and showed a decreasing trend throughout the season (Fig. 1B).

2.2. Stomatal conductance parametrization

As shown in Table 1, g_{max} was higher in clone S than in clone R. T_{max} was the same for both clones, the optimal air tempera-

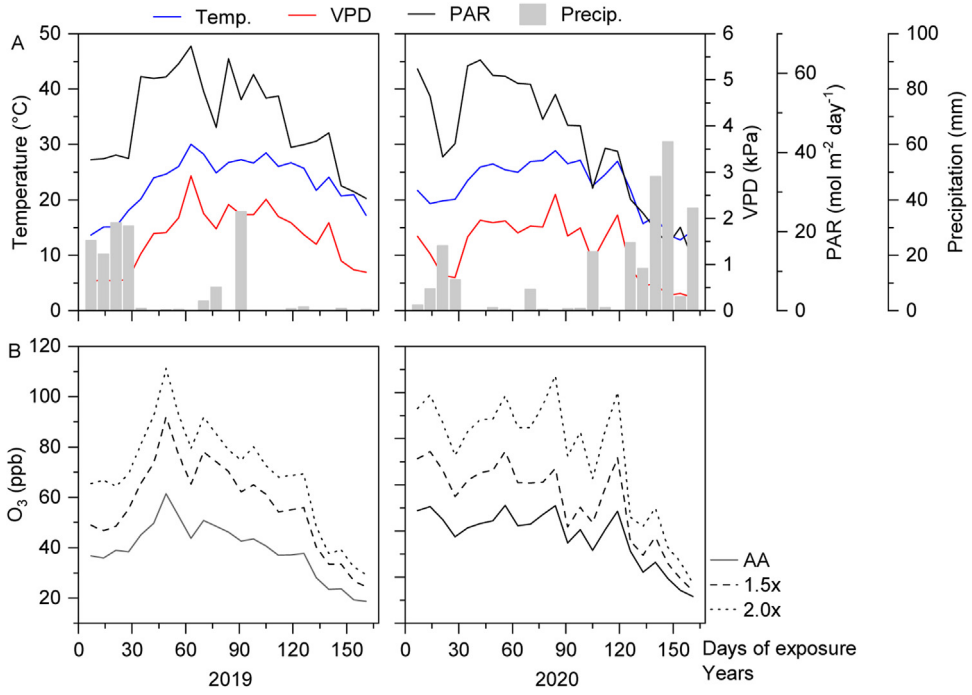

Fig. 1 – (A) Environmental parameters along the experimental period (2019–2020). Daily average of hourly air temperature (Temp.), vapor pressure deficit (VPD), photosynthetic active radiation (PAR) and total daily precipitations. (B) Daily average of O_3 concentrations (ambient air-AA; 1.5 x and 2.0 x) for each year.

Table 1 – Summary of Jarvis-type g_{sto} model parameters for both cypress clones (the CCD resistant clone R - PM 2546 and the CCD sensitive clone S - PM 3375).

Parameter		Unit	Clone R	Clone S
g_{max}		mol O_3/(m^2·sec)	0.087	0.106
f_{min}		fraction	0.164	0.126
f_{temp}	T_{max}	°C	40.0	40.0
	T_{opt}	°C	23.0	23.9
	T_{min}	°C	11.6	10.5
f_{light}	a	constant	0.0030	0.0050
f_{VPD}	VPD_{max}	kPa	2.1	1.6
	VPD_{min}	kPa	4.2	4.0
f_{phen}	A_{start}	day of the year	1	1
	A_{end}	day of the year	365	365
	f_{phen_a}	days	117	101
	f_{phen_b}	days	90	92
	f_{phen_c}	fraction	0.30	0.30
	f_{phen_d}	fraction	0.30	0.30
f_{O3}	q	constant	0.0039	0.0048
f_{canker}	c	constant	0.0410	0.0042
	k	constant	0.2968	0.0648

In detail, g_{max} is the maximum stomatal conductance; f_{min} is the minimum stomatal conductance (fraction); f_{temp}, f_{light}, f_{VPD}, f_{phen}, f_{O3} and f_{canker} are the variation in g_{max} with temperature (T, °C), photosynthetic photon flux density (PPFD, µmol/(m^2·sec)), vapor pressure deficit (VPD, kPa), season, O_3 and canker, respectively. T_{max}, T_{opt}, T_{min}, are the maximum, optimal, and minimum air temperature for stomatal opening while the constant a determines the shape of the exponential relationship in the f_{light} function. VPD_{max} and VPD_{min} are the vapor pressure deficit for attaining maximum and minimum stomatal aperture. A_{start} and A_{end} are the days of start and end of the season. f_{phen_a} and f_{phen_b} are the number of days for f_{phen} to reach its maximum and the number of days during the decline of f_{phen} for the minimum to again be reached, respectively. q represents the stomatal sensitivity to O_3 concentration while c and k are constants linked to stomatal response to bark canker.

Table 2 – Results of the regression analysis between measured and estimated g_{sto} in two cypress clones (clone R and clone S). See Table 1 for the acronym meaning.

Functions	f_{O3}	f_{canker}	Clone R	Clone S
f_{light} ' f_{temp} ' f_{VPD} ' f_{phen}	–	–	$R^2 = 0.39$ $RMSE = 0.022$	$R^2 = 0.32$ $RMSE = 0.033$
f_{light} ' f_{temp} ' $f_{VPD,}$ f_{phen}	+	–	$R^2 = 0.41$ $RMSE = 0.018$	$R^2 = 0.46$ $RMSE = 0.023$
f_{light} ' f_{temp} ' f_{VPD} ' f_{phen}	–	+	$R^2 = 0.43$ $RMSE = 0.021$	$R^2 = 0.33$ $RMSE = 0.032$
f_{light} ' f_{temp} ' f_{VPD} ' f_{phen}	+	+	$R^2 = 0.44$ $RMSE = 0.018$	$R^2 = 0.46$ $RMSE = 0.022$

+ including the function; – not including the function.

ture for stomatal openining (T_{opt}) was higher in clone S, while T_{min} was higher in clone R. The coefficient *a* of the f_{light} function was higher for clone S, which suggests a steeper initial slope of the light response curve in this clone, and the stomatal VPD response was similar between clone R and clone S. As cypress is an evergreen conifer, A_{start} and A_{end} covered the entire year and f_{phen} reached the maximum value between April and September for both clones. Regarding the two additional functions considered in this study, the parameter q for f_{O3} was higher in clone S while clone R showed strongly higher values of constants c and k in f_{canker}. The sensitivity analysis of g_{sto} model parameters demonstrated that, considering only the environmental variables ($f_{light,}$ f_{temp}, f_{VPD} and f_{phen}), clone R showed higher R^2 and lower RMSE than clone S (Table 2). Including both f_{O3} and f_{canker}, however, the model performance improved for both clones with a better fit for clone S. On the other hand, when adding a single variable at a time, clone R provided a better fit with f_{canker} while clone S showed a better performance with only f_{O3}.

Fig. 2A and 2B show g_{sto} response to canker of resistant and susceptible clones at the end of the experiment. f_{canker} suggested a parabolic trend in clone R reaching comparable values of g_{sto} with and without bark necrosis while clone S not recovered g_{sto} in injured clones. Also f_{O3} (Fig. 2C and 2D) showed a different g_{sto} clonal-response to O_3 with a steeper slope for clone S than clone R.

2.3. *Effects on biomass gain*

Ozone decreased *C. sempervirens* biomass gain ($p < 0.001$) (Table 3). Moreover, we found a statistically significant difference in total ($p < 0.001$), aboveground ($p < 0.001$) and belowground ($p < 0.01$) biomass between clones, while inoculation affected total biomass and roots ($p < 0.05$). A significant interaction between clones and O_3 was detected for total and belowground biomass ($p < 0.01$), suggesting that the negative O_3 effects were more evident in Clone S than in Clone R. In addition, we found a significant interaction between inoculation and clone for belowground biomass ($p < 0.05$), which indicates that inoculation induced a reduction of roots only in Clone S (Tukey test, clone S not inoculated *vs.* inoculated; $p < 0.05$). Finally, the interaction of three factors (Inoculation, O_3 and Clone) was significant ($p < 0.05$) for total and aboveground biomass.

2.4. *Exposure and flux-based dose response functions and critical levels detection*

The total B_{ref} values for a theoretical pre-industrial atmosphere, with an O_3 daily concentration of 10 ppb, were similar for not inoculated and inoculated ramets of Clone R (346.4 and 386.3 g, respectively), while not inoculated ramets of Clone S showed a higher value of B_{ref} (487.8 g) than the inoculated ones (394.1 g) (Fig. 3).

Over the two-year experimental period, AOT40 was 48,704.3, 112,984.9 and 176,399.1 ppb·hr, for AA, 1.5 × and 2.0 ×, respectively, while PODy increased with O_3 levels and decreased with increasing y thresholds per both clones (data not shown). Considering all not inoculated ramets together, AOT40 did not respect the first criteria and therefore was excluded from CL calculation. Conversely, PODy showed a statistically significant regression with a C.I. included in Y-intercept = 1 for POD_2 (Fig. 4A) with a $R^2 = 0.85$. The CL corresponding to a total relative biomass loss of 4% was 2.51 mmol/m^2 POD_2 (Fig. 4B). Moreover, CLs were calculated separately for each clone (inoculated and not inoculated). The CLs were found to be 4.24 mmol/m^2 $POD_{1.5}$ (not inoculated) and 2.46 mmol/m^2 POD_1 (inoculated) in clone R, and 1.79 mmol/m^2 $POD_{2.5}$ (not inoculated) and 5.63 mmol/m^2 $POD_{1.5}$ in clone S (inoculated), although dose-response lines were not statistically significant (Appendix A Fig. S1). Taking into account only inoculated ramets together, both criterium was respected for POD_5 for with a CL of 0.15 mmol/m^2 calculated (Fig. 5A), however the regressions were not statistically significant (Fig. 5B).

3. Discussion

3.1. *Stomatal conductance parameterization of C. sempervirens*

This is the first study that assessed the maximum stomatal conductance (g_{max}) of *C. sempervirens*. The values detected (87 and 106 mmol O_3/(m^2·sec) for Clone R and S, respectively), although slightly higher, were in agreement with the value reported by Hoshika et al. (2018d) for boreal/temperate needle leaved evergreen trees (0.12 mol H_2O/(m^2·sec) equal to 80 mmol O_3/(m^2·sec)). Nevertheless, they resulted lower than the g_{max} recorded for other Meditteranean conifers such as Pi-

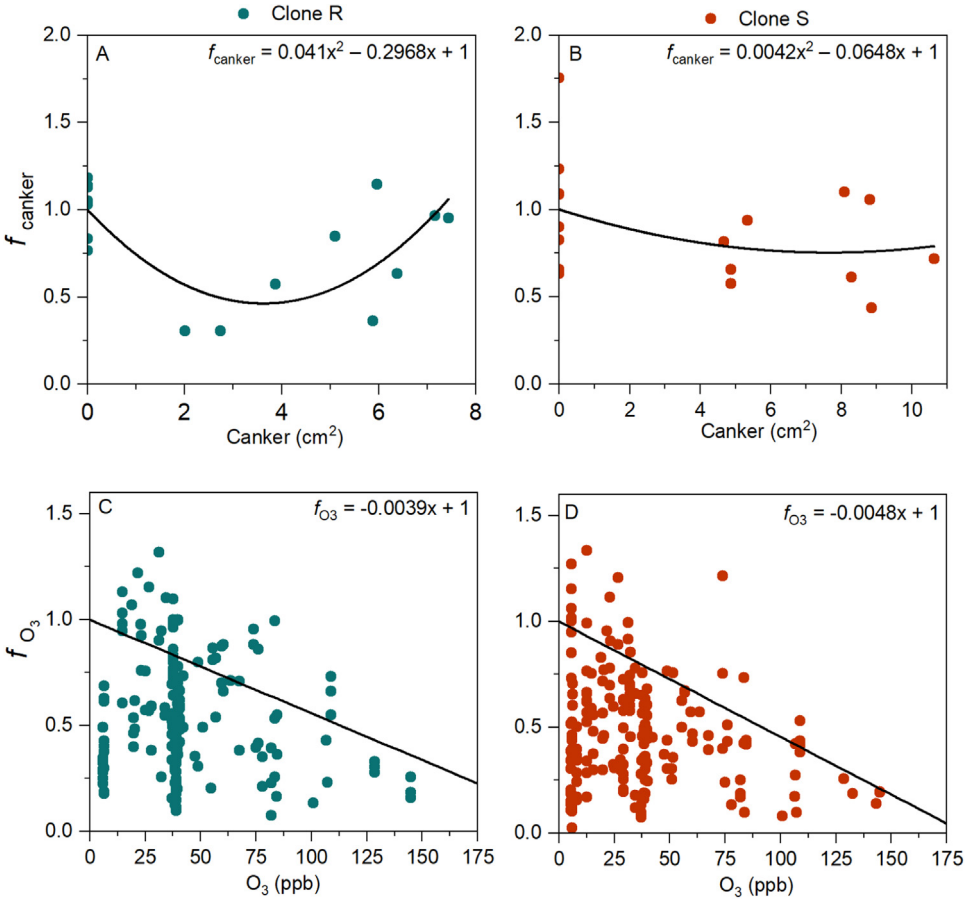

Fig. 2 – (A) Stomatal conductance response to canker lesion area for CCD-Resistant clones of *C. sempervirens* (*n* = 18), (B) stomatal conductance response to canker lesion area for CCD-Susceptible clones of *C. sempervirens* (*n* = 18), (C) stomatal conductance response to O_3 for CCD-Resistant clones of *C. sempervirens* (*n* = 198), (D) stomatal conductance response to O_3 for CCD-Susceptible clones of *C. sempervirens* (*n* = 204).

nus pinea (145 mmol O_3/(m^2·sec); Moura et al., 2022) and *Pinus halepensis* (230 mmol O_3/(m^2·sec); CLRTAP, 2017). Also the g_{max} of other conifers typical of colder climates i.e., *Pinus sylvestris* (180 mmol O_3/(m^2·sec); Emberson et al., 2007), *Larix kaempferi* (average 130 mmol O_3/(m^2·sec); Hoshika et al., 2020a), *Picea abies* (130 mmol O_3/(m^2·sec); Moura et al., 2022) and *Pinus mugo* (110 mmol O_3/(m^2·sec); Bičárová et al., 2019), was higher than that of *C. sempervirens* confirming that this species can be considered as a water saving species, well resistant to drought and well adapted to Mediterranean climatic extremes (Froux et al., 2002, 2005; Caudullo and De Rigo, 2016).

For stomatal conductance parameterization we used the simplistic Jarvis scheme rather than the biochemical-based Ball-Berry. Both algorithms show similar performances for g_{sto} modelling and need a site-specific parameterization accounting for local growing conditions (Büker et al., 2007). Nonetheless, Ball-Berry has higher input requirements (V_{cmax},J_{max} and *m*) compared to Jarvis (only g_{max}) and for this reason we decided to adopt this multiplicative algorithm.

The two functions (f_{O3} and f_{canker}), proposed in this study, improved the fitting of estimated stomatal conductance to the measured value for both clones, suggesting that O_3 and *S. cardinale* infection have the capacity to affect stomatal regulation (see Table 2). In particular, f_{canker} showed a different behavior between Clone S and Clone R. As shown in Fig. 2A and 2B, Clone S responded to pathogen infection by losing its stomatal functionality. Interestingly, pathogen-induced stomatal deregulation was previously observed e.g. in *Vitis vinifera*, *Eucalyptus globosus* and *Quercus robur* leaves affected by *Plasmopara viticola* (Allègre et al., 2007), *Mycosphaerella* species (Pinkard and Mohammed, 2006) and *Erysiphe alphitoides* (Hajii et al., 2009), respectively. However, the above-mentioned pathogens carry out their pathogenic activity on leaf tissues and it is more plausible that g_{sto} was affected, while it is surprising how CCD can influence g_{sto} being a bark pathogen. In contrast, Clone R showed a recovery of g_{sto} after an initial decline, and ramets with more extensive necrosis reached values similar to the not inoculated ones, suggesting that infection did not significantly alter gas exchanges in this clone. The function f_{O3} (Fig. 2C and 2D) underlined a higher stomatal sensitivity to O_3 for Clone S than Clone R (steeper slope and consequently higher q parameter).

Our findings suggest that Clone S is less tolerant to O_3 stress and defends itself by implementing a stomatal closing mechanism (avoidance). This eco-physiological behaviour was already documented in other tree species characteristic

Table 3 – Total, aboveground and belowground biomass gain (average ± standard error) of *C. sempervirens* clones (clone R - PM 2546 and clone S - PM 3375), exposed to three O_3 treatments (AA, 1.5 x and 2.0 x) and inoculated or not inoculated with *Seiridium cardinale*.

	Clone	O_3 treatments	Total biomass (g)	Aboveground biomass (g)	Belowground biomass (g)
Not inoculated	R	AA	301.72 ± 11.44 ab	195.66 ± 19.47 ab	106.06 ± 9.83 a
		1.5×	321.12 ± 15.26 a	227.23 ± 8.90 a	93.89 ± 6.94 a
		2.0×	259.14 ± 6.38 b	171.13 ± 1.57 b	88.01 ± 6.14 a
	S	AA	370.12 ± 7.65 α	246.98 ± 2.91 α	123.15 ± 5.74 α
		1.5×	394.14 ± 23.37 α	264.91 ± 19.70 α	129.23 ± 5.27 α
		2.0×	278.98 ± 19.35 β	181.07 ± 14.55 β	97.91 ± 4.82 β
Inoculated	R	AA	319.97 ± 23.18 A	206.98 ± 15.32 A	112.98 ± 11.28 A
		1.5×	283.68 ± 7.89 A	194.62 ± 10.08 A	89.06 ± 3.22 AB
		2.0×	244.43 ± 24.40 A	162.43 ± 24.88 A	82.01 ± 1.76 B
	S	AA	293.39 ± 10.69 α'	191.08 ± 3.08 α'	102.31 ± 9.03 $\alpha'\beta$'
		1.5×	390.37 ± 7.70 β'	274.60 ± 1.17 β'	115.78 ± 8.33 α'
		2.0×	263.26 ± 17.24 α'	188.36 ± 13.64 α'	74.90 ± 4.76 β'
Three-way ANOVA					
O_3			***	***	***
Clone			***	***	**
Inoculation			*	n.s.	*
O_3 × Inoculation			n.s.	n.s.	n.s.
O_3 × Clone			**	n.s.	**
Inoculation × Clone			n.s.	n.s.	*
Inoculation × Clone × O_3			*	*	n.s.

Different letters (a, b, A, B, α, β, α', β') indicate significant differences among O_3 treatments for each inoculated or not inoculated clone (R or S) following three-way ANOVA and Tukey test (n.s. not significant, * $p < 0.05$, ** $p < 0.01$, *** $p < 0.001$, $n = 3$).

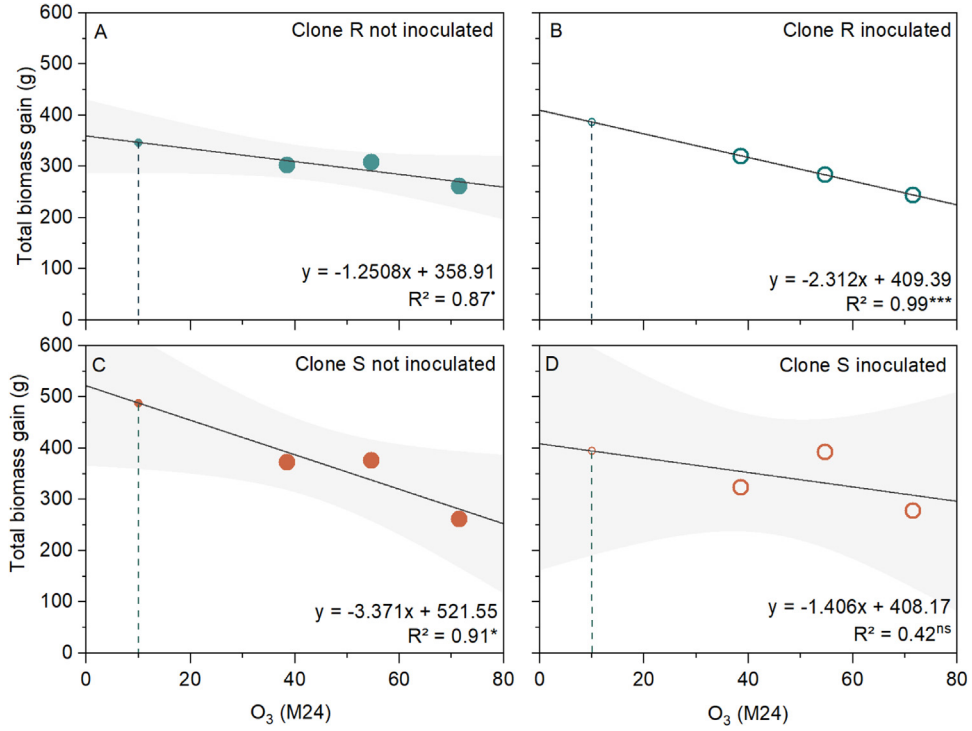

Fig. 3 – Response of total biomass gain of two *C. sempervirens* clones (clone R - PM 2546 and clone S - PM 3375) with different inoculation treatments (inoculated and not inoculated) exposed to different O_3 levels (M24 is the daily average), as obtained by fumigating ramets to AA, 1.5 x and 2.0 x. The dotted line represents the biomass calculated for a clean air pre-industrial level of O_3 concentration (10 ppb). Gray zones show a 95% confidence interval.

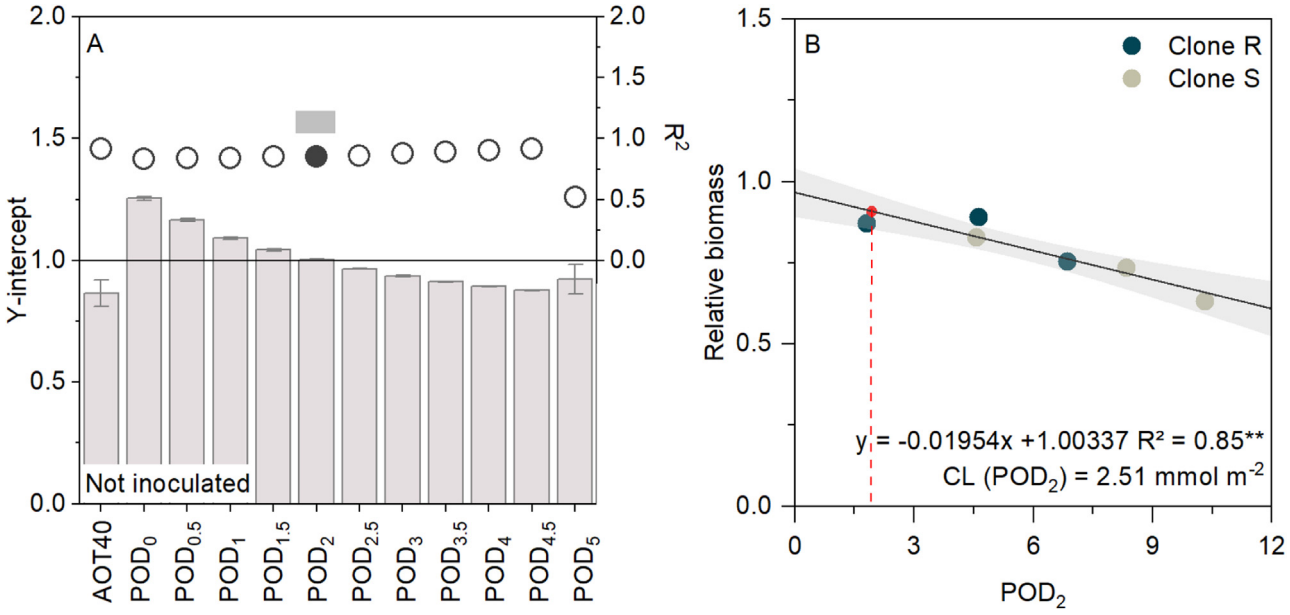

Fig. 4 – (A) Coefficients of determination (R^2) represented by dots and Y-intercepts represented by bars (± C.I.), obtained from linear regressions between relative biomass loss for cypress clones (both clones R and S were considered) and ozone metrics, i.e., AOT40 and PODy with y thresholds from 0 to 5 nmol O_3/(m^2•sec). The horizontal line represents the Y-intercept = 1 and the grey bar on top of the graph represents the Y range where C.I. of the intercept includes 1. The black dot indicates the highest R^2 within the range where the intercept includes 1. (B) Linear regression between POD_2 and relative biomass, and critical level (in red) corresponding to a biomass loss of 4%.

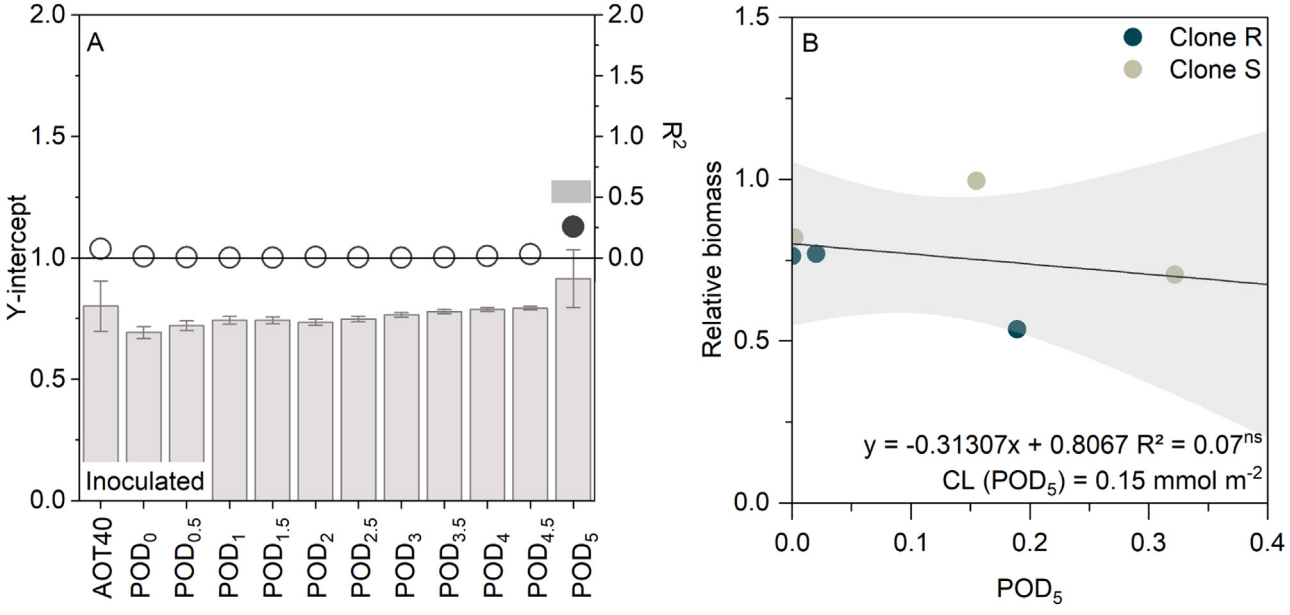

Fig. 5 – (A) Coefficients of determination (R^2) represented by dots and Y-intercepts represented by bars (± C.I.), obtained from linear regressions between relative biomass loss for *S. cardinale* inoculated cypress clones (clones R and S together) and ozone metrics, i.e., AOT40 and PODy with y thresholds considered (from 0 to 5). The horizontal line represents the Y-intercept = 1 and the grey bar on top of the graph represents the Y range where C.I. of the intercept includes 1. The black dot indicates the highest R^2 within the range where the intercept includes 1. B) Linear regression between POD_5 and relative biomass for inoculated *C. sempervirens*.

of Mediterranean forests i.e., *Phillyrea angustifolia* and *Quercus robur* (Hoshika et al., 2020a) or belonging to the genus *Acer* (Calatayud et al., 2007). Ozone exposure could have induced high levels of Reactive Oxygen Species (ROS) in Clone S twigs. Indeed, previous studies reported as ROS are an important component of the phytohormone abscisic acid (ABA) signaling pathway in guard cells leading to stomatal closure (Kangasjärvi et al., 2005; McAdam et al., 2017). Conversely, Clone R was able to tolerate high concentrations of O_3 similarly to other xerophytic woody species (e.g., *Quercus ilex* and *Q. pubescens*; Hoshika et al., 2020b). These species developed leaf anatomical features (e.g., thick cuticle and waxes) to counteract oxidative stressors, such as water deficit and the excess of UV radiation, typical of the Mediterranean region. In addition, they are equipped with an active antioxidant pool, which may also work for the detoxification of O_3 within the mesophyll (Paoletti, 2006). Furthermore, the lower g_{max} showed by Clone R than Clone S could allow a reduced O_3 uptake and a consequently better detoxifying capacity (Matyssek et al., 2008).

3.2. *Ozone risk assessment and biomass gain reduction*

We recommended the flux-based index (PODy) rather than the exposure-based index (AOT40) for *C. sempervirens* O_3 risk assessment. Indeed, AOT40 did not respect the criteria to calculate the CL for total biomass. Other authors confirmed that for young trees exposed under experimental conditions, impact on biomass could be better explained using accumulated stomatal O_3 flux such as PODy rather than AOT40 (Gao et al., 2017; Hoshika et al., 2018c; Moura et al., 2021). In detail, we found that 2 nmol $O_3/(m^2 \cdot sec)$ (POD_2) was the best y threshold to assess total biomass reduction for *C. sempervirens* (plotting all not inoculated ramets together) with a CL of 2.51 mmol/m^2 POD_2. However, CLRTAP (2017) suggests to calculate CL with a y threshold of 1 nmol/$(m^2 \cdot sec)$ (POD_1) for forest tree species. If POD_1 was chosen for *C. sempervirens*, CL would be 3.94 mmol/m^2 (data not shown), i.e. lower than the value (4.31 mmol/m^2) recorded for another conifer such as Japanese larch (*Larix kaempferi*, Hoshika et al., 2020a). Therefore, *C. sempervirens* seems to be highly sensitive to O_3 according to POD_1-based CLs but it should be considered that this species showed a high avoidance capacity against O_3 damage as confirmed by the low stomatal conductance thus limiting stomatal O_3 uptake. Kohno et al. (2005) conducted experiments in open-top chambers on species belonging to *Cupressaceae* family (i.e., *Cryptomeria japonica* and *Chamaecyparis obtusa*) and found AOT40-based CLs > 31,000 ppb·hr, corresponding to 10% reduction of whole-plant dry mass during the growing season (6 months), and categorizing these species as low sensitivity for O_3. Considering the dose-response relationship between AOT40 and relative total biomass for *C. sempervirens*, the CL, equal to 10% reduction, was 71,592 ppb·hr (data not shown) which indicates common cypress as an O_3-resistant species. To confirm this, if we considered a biomass reduction of 5%, as suggested by CLRTAP (2017) to detect AOT40-based CL for trees, we found a value of 35,796 ppb·hr (data not shown), that is seven times higher of the limit purposed by CLRTAP (2017) (5000 ppb·hr). In addition, Karlsson et al. (2004) found a CL of 4700 ppb·hr AOT40 equal to a biomass reduction of 0.8% for sensitive conifer species such as Norway spruce (*Picea abies*) and Scots pine (*Pinus sylvestris*) but, also in this case, our results showed a higher value (5727 ppb·hr; data not shown) suggesting *C. sempervirens* as a conifer more resistant to O_3.

A negative O_3-effect on total and root biomass for Clone S was detected at the end of the experiment. Decrease of root biomass in plants exposed to O_3 is a very common and well documented phenomenon (Gu et al., 2023). Among conifers, *Pinus uncinata* saplings highlighted similar results with reduction of root biomass under increased exposure to O_3 during a two-year free-air O_3 fumigation (Díaz-de-Quijano et al., 2012). Probably, our result was related to a higher carbon demand in the twigs for antioxidants synthesis involved in ROS detoxification while Clone R maybe possessed a more efficient antioxidant pool. Furthermore, we found a significative belowground biomass reduction due to inoculation in Clone S. It is possible to hypothesize a change in carbon allocation from roots towards stems where infections were located. In fact, cypress could shift more photosynthates from the primary towards the secondary metabolism, favoring the synthesis of compounds involved in the defense against *Seiridium cardinale* such as polyphenols, terpenes and suberin (Achotegui-Castells et al., 2015, 2016; Danti et al., 2018; Della Rocca et al., 2021).

Root biomass reduction and a higher shoot/root ratio for plants exposed to O_3 (Andersen, 2003; Grantz et al., 2006; Carriero et al., 2015; Li et al., 2020) are dangerous, especially for species, such as cypress, commonly used in urban greening since trees could lose stability undergoing overturning under windstorm increasingly frequent due to climate change (Giachetti et al., 2021). Moreover, this detrimental effect on belowground biomass can aggravate cypress susceptibility to other stressors typical of the Mediterranean environment such as summer drought and nutrient availability due to impairment of root function (Sardans and Peñuelas, 2013).

Significant O_3 dose-response relationships were not found for the inoculated *C. sempervirens* ramets (clone R and S plotted together). In Clone R, the biomass growth reduction induced by *S. cardinale* was unaffected by 1.5 × O_3 exposure while an additive effect was detected at 2.0 × although it was not significant. Conversely, in Clone S the 1.5 × O_3 exposure significantly counteracted the biomass loss promoted by inoculation. Therefore, Clone S could be lacking in defensive biochemical tools (or have a lower ability to use them) to face both stressors and, in presence of moderate O_3 fumigation (1.5 ×), may have invested in growth to synthetize these compounds (hormetic response; Agathokleous et al., 2019). Instead, Clone R could be already provided with such compounds thus avoiding biomass increment under O_3 1.5 ×. However, as a whole, our results showed that additive biotic stress induced by *S. cardinale* masked the effect of O_3 stress on *C. sempervirens* biomass thus changing O_3 risk assessment.

4. Conclusions

Ozone risk assessment for *C. sempervirens* was explored for the first time leading to the recommendation of PODy-based CLs, while the exposure-based index AOT40 was not found to be suitable for predicting O_3 impacts on cypress biomass. Our re-

sults suggest 2.51 mmol/m^2 POD_2 as CL not to exceed a 4% loss of total relative biomass. Interestingly, we found that O_3 risk assessment was not aggravated by the biotic stress induced by *S. cardinale* as inoculated Clone S ramets showed a significant biomass increase under medium level O_3 (1.5 ×) thus masking the negative O_3 effect. Moreover, we discovered that a different intra-specific response to O_3 depended on the sensitivity to a biotic stress, i.e. the *S. cardinale* infection. Indeed, Clone S showed a higher reduction of biomass (total and belowground) than Clone R for both stressors. Therefore, the more tolerant clone R may be recommended for facing future climate change scenarios, characterized by high concentrations of tropospheric O_3. Nevertheless, further studies are needed to assess if this different carbon allocation in Clone S is linked to the secondary metabolism compounds involved in the defense against O_3 and *S. cardinale*. In addition, although experiments conducted in FACE facilities provide more realistic results than those obtained in Open Top Chamber, a thorough analysis on effects of long-term O_3 exposure on this species could be still worthwhile to validate and update our findings.

Our results help protect an iconic species of the Mediterranean area, and preserve its ornamental function as well as other important ecosystem services e.g., timber production, windbreaks barrier and erosion control.

Declaration of Competing Interest

The authors declare that they have no known competing financial interests or personal relationships that could have appeared to influence the work reported in this paper.

Acknowledgements

This work was supported by the Italian Integrated Environmental Research Infrastructures Systems (ITINERIS) (Nos. IR0000032, CUP B53C22002150006). Moreover, we would like to thank Alessandro Materassi for maintenance and data validation of O_3 FACE, Moreno Lazzara for field work, Sofia Martini and Andrea Ingrasciotta for biomass assessment as well as Anna Pugliese and Matilde Diani for support in creating the graphs.

Supplementary materials

Supplementary material associated with this article can be found in the online version at doi:10.1016/j.jes.2024.03.026.

References

Achotegui-Castells, A., Danti, R., Llusià, J., Rocca, G.D., Barberini, S., Peñuelas, J., 2015. Strong induction of minor terpenes in Italian cypress, *cupressus sempervirens*, in response to infection by the fungus *Seiridium cardinale*. J. Chem. Ecol. 41, 224–243.

Achotegui-Castells, A., Della Rocca, G., Llusià, J., Danti, R., Barberini, S., Bouneb, M., et al., 2016. Terpene arms race in the *Seiridium cardinale–cupressus sempervirens* pathosystem. Sci. Rep. 6 (1), 1–13.

Agathokleous, E., Belz, R.G., Calatayud, V., De Marco, A., Hoshika, Y., Kitao, M., et al., 2019. Predicting the effect of ozone on vegetation via linear non-threshold (LNT), threshold and hormetic dose- response models. Sci. Total Environ. 649, 61–74.

Ahmed, S., 2007. Impact of air pollution on plant diseases–a review. *Pakistan J. Phytopathol* 19, 192–198.

Allègre, M., Daire, X., Héloir, M.C., Trouvelot, S., Mercier, L., Adrian, M., et al., 2007. Stomatal deregulation in *Plasmopara viticola*-infected grapevine leaves. New Phytol. 173 (4), 832–840.

Andersen, C.P., 2003. Source–sink balance and carbon allocation below ground in plants exposed to ozone. New Phytol. 157 (2), 213–228.

Ben Rejeb, I., Pastor, V., Mauch-Mani, B., 2014. Plant responses to simultaneous biotic and abiotic stress: molecular mechanisms. Plants 3 (4), 458–475.

Bičárová, S., Sitková, Z., Pavlendová, H., Fleischer Jr, P., Fleischer Sr, P., Bytnerowicz, A., 2019. The role of environmental factors in ozone uptake of *Pinus mugo* Turra. Atmos. Pollut. Res. 10 (1), 283–293.

Braun, S., Schindler, C., Leuzinger, S., 2010. Use of sap flow measurements to validate stomatal functions for mature beech (Fagus sylvatica) in view of ozone uptake calculations. Environ. Pollut. 158, 2954–2963.

Büker, P., Emberson, L.D., Ashmore, M.R., Cambridge, H.M., Jacobs, C.M.J., Massman, W.J., et al., 2007. Comparison of different stomatal conductance algorithms for ozone flux modelling. Environ. Pollut. 146 (3), 726–735.

Büker, P., Feng, Z., Uddling, J., Briolat, A., Alonso, R., Braun, S., et al., 2015. New flux based dose-response relationships for ozone for European forest tree species. Environ. Pollut. 206, 163–174.

Calatayud, V., Cerveró, J., Sanz, M.J., 2007. Foliar, physiological and growth responses of four maple species exposed to ozone. Water Air Soil Pollut. 185, 239–254.

Carriero, G., Emiliani, G., Giovannelli, A., Hoshika, Y., Manning, W.J., Traversi, M.L., et al., 2015. Effects of long-term ambient ozone exposure on biomass and wood traits in poplar treated with ethylenediurea (EDU). Environ. Pollut. 206, 575–581.

Caudullo, G., De Rigo, D., 2016. *Cupressus Sempervirens* in Europe: distribution, habitat, usage and threats. European atlas of forest tree species. Publications Office of the European Union, Luxembourg, p. e015be7.

Chaudhry, S., Sidhu, G.P.S., 2022. Climate change regulated abiotic stress mechanisms in plants: a comprehensive review. Plant Cell Rep. 41 (1), 1–31.

CLRTAP, 2015. Mapping critical levels for vegetation. chapter III of manual on methodologies and criteria for modelling and mapping critical loads and levels and air pollution effects. risks and trends. UNECE convention on long-range transboundary air pollution; accessed on 25 Feb 2023 on Web at. www.icpmapping.org.

CLRTAP, 2017. Mapping critical levels for vegetation, chapter III of manual on methodologies and criteria for modelling and mapping critical loads and levels and air pollution effects, risks and trends. UNECE convention on long-range transboundary air pollution; accessed on 01st March 2023 on Web at www.icpmapping.org.

Danti, R., Panconesi, A., Di Lonardo, V., Della Rocca, G., Raddi, P., 2006. 'Italico' and 'Mediterraneo': two *Seiridium cardinale* Canker-Resistant Cypress Cultivars of *Cupressus sempervirens*. HortScience 41 (5), 1357–1359.

Danti, R., Della Rocca, G., Di Lonardo, V., Pecchioli, A., Raddi, P., 2011. Genetic improvement program of cypress: results and outlook", status of the experimental network of mediterranean forest genetic resources. Silva Mediterranea 89–96 Rome, Italy.

Danti, R., Della Rocca, G., Panconesi, A., 2013a. "Cypress Canker", CAB International, 359–375.

Danti, R., Di Lonardo, V., Pecchioli, A., Della Rocca, G., 2013b. Le Crete 1'and 'Le Crete 2': two newly patented *Seiridium cardinale* canker-resistant cultivars of *Cupressus sempervirens*. For. Pathol. 43 (3), 204–210.
Danti, R., Della Rocca, G., 2017. Epidemiological history of cypress canker disease in source and invasion sites. Forests 8 (4), 121.
Danti, R., Rotordam, M.G., Emiliani, G., Giovannelli, A., Papini, A., Tani, C., et al., 2018. Different clonal responses to cypress canker disease based on transcription of suberin-related genes and bark carbohydrates' content. Trees 32, 1707–1722.
Della Rocca, G., Eyre, C.A., Danti, R., Garbelotto, M., 2011a. Sequence and simple-sequence repeat analyses of the fungal pathogen *Seiridium cardinale* indicate california is the most likely source of the Cypress canker epidemic for the mediterranean region. Phytopathology 101 (12), 1408–1417.
Della Rocca, G., Di Lonardo, V., Danti, R., 2011b. Newly-assessed fungicides for the control of cypress canker caused by Seiridium cardinale. Phytopathol. Mediterr. 50 (1), 66–74.
Della Rocca, G., Osmundson, T., Danti, R., Doulis, A., Pecchioli, A., Donnarumma, F., et al., 2013. AFLP analyses of California and Mediterranean populations of *Seiridium cardinale* provide insights on its origin, biology and spread pathways. For. Pathol. 43 (3), 211–221.
Della Rocca, G., Danti, R., Popenuck, T., Di Lonardo, V., Garbelotto, M., 2018. Resistance to cypress canker disease in Italian cypress has desirable effects on disease epidemiology, but may fail against novel genotypes of the pathogen *Seiridium cardinale*. For. Ecol. Manage. 424, 259–266.
Della Rocca, G., Luchi, N., Danti, R., Santini, A., 2019a. Effects of global change on forest diseases and indirect implications in water cycle. Sustain. Agric. Water Manag. 48–61.
Della Rocca, G., Danti, R., Williams, N., Eyre, C., Garbelotto, M., 2019b. Molecular analyses indicate that both native and exotic pathogen populations serve as sources of novel outbreaks of cypress canker disease. Biol. Invasions 21 (9), 2919–2932.
Della Rocca, G., Posarelli, I., Morandi, F., Tani, C., Barberini, S., Danti, R., et al., 2021. Different polyphenolic parenchyma cell and phloem axial resin duct-like structure formation rates in cupressus sempervirens clones infected with Seiridium cardinale. Plant Dis. 105 (10), 2801–2808.
Díaz-de-Quijano, M., Schaub, M., Bassin, S., Volk, M., Peñuelas, J., 2012. Ozone visible symptoms and reduced root biomass in the subalpine species *Pinus uncinata* after two years of free-air ozone fumigation. Environ. Pollut. 169, 250–257.
Dusenge, M.E., Duarte, A.G., Way, D.A., 2019. Plant carbon metabolism and climate change: elevated CO2 and temperature impacts on photosynthesis, photorespiration and respiration. New Phytol. 221 (1), 32–49.
Easlon, H.M., Bloom, A.J., 2014. Easy Leaf Area: automated digital image analysis for rapid and accurate measurement of leaf area. Appl. Plant Sci. 2, 1400033.
Emberson, L.D., Ashmore, M.R., Cambridge, H.M., Simpson, D., Tuovinen, J.P., 2000. Modelling stomatal ozone flux across Europe. Environ. Pollut. 109 (3), 403–413.
Emberson, L.D., Büker, P., Ashmore, M.R., 2007. Assessing the risk caused by ground level ozone to European forest trees: a case study in pine, beech and oak across different climate regions. Environ. Pollut. 147 (3), 454–466.
European Council Directive, 2008. 2008/50/EC of the European Parliament and of the council of 21st May 2008 on ambient air quality and cleaner air for Europe. Official Journal L 152, 1–44.
Farahmand, H., 2020. The genus *Cupressus* L.: mythology to biotechnology with emphasis on mediterranean cypress (*Cupressus sempervirens* L.). Hortic Rev. (Am Soc. Hortic. Sci.) 47, 213–287.
Fowler, D., 2008. Ground-level Ozone in the 21st century: future trends. impacts and policy implications. The Royal Society, London.
Froux, F., Huc, R., Ducrey, M., Dreyer, E., 2002. Xylem hydraulic efficiency versus vulnerability in seedlings of four contrasting mediterranean tree species (*Cedrus atlantica, Cupressus sempervirens, Pinus halepensis* and *Pinus nigra*). Ann. For. Sci. 59 (4), 409–418.
Froux, F., Ducrey, M., Dreyer, E., Huc, R., 2005. Vulnerability to embolism differs in roots and shoots and among three Mediterranean conifers: consequences for stomatal regulation of water loss? Trees 19, 137–144.
Gao, F., Catalayud, V., Paoletti, E., Hoshika, Y., Feng, Z., 2017. Water stress mitigates the negative effects of ozone on photosynthesis and biomass in poplar plants. Environ. Pollut. 230, 268–279.
Giachetti, A., Ferrini, F., Bartoli, G., 2021. A risk analysis procedure for urban trees subjected to wind-or rainstorm. Urban Forestry & Urban Greening 58, 126941.
Graniti, A., 1998. CYPRESS CANCKER: a Pandemic in Progress. Annual Reviews Phytopathology 36, 91–114.
Grantz, D.A., Gunn, S., Vu, H.B., 2006. O_3 impacts on plant development: a meta-analysis of root/shoot allocation and growth. Plant Cell Environ. 29 (7), 1193–1209.
Grulke, N.E., Heath, R.L., 2020. Ozone effects on plants in natural ecosystems. Plant Biol. 22, 12–37.
Gu, X., Wang, T., Li, C., 2023. Elevated ozone decreases the multifunctionality of belowground ecosystems. Glob. Chang. Biol. 29 (3), 890–908.
Hajji, M., Dreyer, E., Marçais, B., 2009. Impact of *Erysiphe alphitoides* on transpiration and photosynthesis in *Quercus robur* leaves. Eur. J. Plant Pathol. 125, 63–72.
Hayes, F., Williamson, J., Mills, G., 2015. Species-specific responses to ozone and drought in six deciduous trees. Water Air Soil Pollut. 226 (5), 156.
Hoshika, Y., Paoletti, E., Omasa, K., 2012. Parameterization of Zelkova serrata stomatal conductance model to estimate stomatal ozone uptake in Japan. Atmos. Environ. 55, 271–278.
Hoshika, Y., Watanabe, M., Carrari, E., Paoletti, E., Koike, T., 2018a. Ozone-induced stomatal sluggishness changes stomatal parameters of Jarvis-type model in white birch and deciduous oak. Plant Biol. 20 (1), 20–28.
Hoshika, Y., Moura, B., Paoletti, E., 2018b. Ozone risk assessment in three oak species as affected by soil water availability. Environ. Sci. Pollut. Res. 25, 8125–8136.
Hoshika, Y., Moura, B., Paoletti, E., 2018c. Ozone risk assessment in three oak species as affected by soil water availability. Environ. Sci. Pollut. Res. 25, 8125–8136.
Hoshika, Y., Osada, Y., De Marco, A., Penuelas, J., Paoletti, E., 2018d. Global diurnal and nocturnal parameters of stomatal conductance in woody plants and major crops. Global Ecol. Biogeogr. 27 (2), 257–275.
Hoshika, Y., Paoletti, E., Agathokleous, E., Sugai, T., Koike, T., 2020a. Developing ozone risk assessment for larch species. Front. For. Glob. Change 3, 45.
Hoshika, Y., Fares, S., Pellegrini, E., Conte, A., Paoletti, E., 2020b. Water use strategy affects avoidance of ozone stress by stomatal closure in mediterranean trees—a modelling analysis. Plant Cell Environ. 43 (3), 611–623.
Jarvis, P.G., 1976. Interpretation of variations in leaf water potential and stomatal conductance found in canopies in field. Phil. Trans. R. Soc. Lond. B 273, 593–610.
Jiang, J., Aksoyoglu, S., Ciarelli, G., Baltensperger, U., Prévôt, A.S., 2020. Changes in ozone and PM2.5 in Europe during the period of 1990–2030: role of reductions in land and ship emissions. Sci. Total Environ. 741, 140467.
Kangasjärvi, J., Jaspers, P., Kollist, H., 2005. Signalling and cell death in ozone-exposed plants. Plant Cell Environ. 28, 1021–1036.
Karlsson, P.E., Uddling, J., Braun, S., Broadmeadow, M., Elvira, S., Gimeno, B.S., et al., 2004. New critical levels for ozone effects

on young trees based on AOT40 and simulated cumulative leaf uptake of ozone. Atmos. Environ. 38 (15), 2283–2294.
Kohno, Y., Matsumura, H., Ishii, T., Izuta, T., 2005. Establishing critical levels of air pollutants for protecting East Asian vegetation—a challenge. Plant responses to air pollution and global change 243–250.
Li, P., Yin, R., Shang, B., Agathokleous, E., Zhou, H., Feng, Z., 2020. Interactive effects of ozone exposure and nitrogen addition on tree root traits and biomass allocation pattern: an experimental case study and a literature meta-analysis. Sci. Total Environ. 710, 136379.
McAdam, E.L., Brodribb, T.J., McAdam, S.A., 2017. Does ozone increase ABA levels by non-enzymatic synthesis causing stomata to close? Plant Cell Environ. 40 (5), 741–747.
Madar, Z., Solel, Z., Sztejnberg, A., 1990. The effect of Diplodia pinea f. sp. cupressi and Seiridium cardinale on water flow in cypress branches. Physiol. Mol. Plant Pathol. 37 (5), 389–398.
Matyssek, R., Sandermann, H., Wieser, G., Booker, F., Cieslik, S., Musselman, R., et al., 2008. The challenge of making ozone risk assessment for forest trees more mechanistic. Environ. Pollut. 156 (3), 567–582.
Montes, C.M., Demler, H.J., Li, S., Martin, D.G., Ainsworth, E.A., 2022. Approaches to investigate crop responses to ozone pollution: from O3-FACE to satellite-enabled modeling. Plant J. 109 (2), 432–446.
Moura, B.B., Brunetti, C., da Silva Engela, M.R.G., Hoshika, Y., Paoletti, E., Ferrini, F., 2021. Experimental assessment of ozone risk on ecotypes of the tropical tree *Moringa oleifera*. Environ. Res. 201, 111475.
Moura, B.B., Carrari, E., Dalstein-Richier, L., Sicard, P., Leca, S., Badea, O., et al., 2022. Bridging experimental and monitoring research for visible foliar injury as bio-indicator of ozone impacts on forests. Ecosystem Health and Sustainability 8 (1), 2144466.
Ochoa-Hueso, R., Munzi, S., Alonso, R., Arróniz-Crespo, M., Avila, A., Bermejo, V., et al., 2017. Ecological impacts of atmospheric pollution and interactions with climate change in terrestrial ecosystems of the Mediterranean Basin: current research and future directions. Environ. Pollut. 227, 194–206.
Naz, S., Fatima, Z., Iqbal, P., Khan, A., Zakir, I., Ullah, H., et al., 2022. An introduction to climate change phenomenon. Building Climate Resilience in Agriculture: Theory, Practice and Future Perspective 3–16.
Panconesi, A., Raddi, P., 1991. Agrimed No. 1 and Bolgheri: two new cypress varieties resistant to canker. Cellulosa e Carta 42 (1), 47–52.
Paoletti, E., 2006. Ozone impacts on mediterranean forests: a review. Environ. Pollut. 144, 463–474.
Paoletti, E., Materassi, A., Fasano, G., Hoshika, Y., Carriero, G., Silaghi, D., et al., 2017. A new-generation 3D ozone FACE (free air controlled exposure). Sci. Total Environ. 575, 1407–1414.
Paoletti, E., Sicard, P., Hoshika, Y., Fares, S., Badea, O., Pitar, D., et al., 2022. Towards long-term sustainability of stomatal ozone flux monitoring at forest sites. Sustainable Horizons 2, 100018.
Pinkard, E.A., Mohammed, C.L., 2006. Photosynthesis of *eucalyptus globulus* with *mycosphaerella* leaf disease. New Phytol. 170 (1), 119–127.
Raddi, P., Panconesi, A., 1981. Cypress canker disease in Italy: biology, control possibilities and genetic improvement for resistance. European Journal of Forest Pathology 11 (5–6), 340–347.
Roeber, V.M., Bajaj, I., Rohde, M., Schmülling, T., Cortleven, A., 2021. Light acts as a stressor and influences abiotic and biotic stress responses in plants. Plant Cell Environ. 44 (3), 645–664.
Sardans, J., Peñuelas, J., 2013. Plant-soil interactions in Mediterranean forest and shrublands: impacts of climatic change. Plant Soil 365, 1–33.
Sicard, P., Anav, A., De Marco, A., Paoletti, E., 2017. Projected global tropospheric ozone impacts on vegetation under different emission and climate scenarios. Atmos. Chem. Phys. 17 (19), 12177–12196.
Trivedi, P., Batista, B.D., Bazany, K.E., Singh, B.K., 2022. Plant–microbiome interactions under a changing world: responses, consequences and perspectives. New Phytol. 234 (6), 1951–1959.
Vainonen, J.P., Kangasjärvi, J., 2015. Ozone action on plants. Plant Cell Environ. 38, 240–252.
Zandalinas, S.I., Fritschi, F.B., Mittler, R., 2021. Global warming, climate change, and environmental pollution: recipe for a multifactorial stress combination disaster. Trends Plant Sci. 26 (6), 588–599.